ELSEVIER

International Journal of Heat and Fluid Flow 23 (2002) 647–656

International Journal of HEAT AND FLUID FLOW

www.elsevier.com/locate/ijhff

Experimental studies and modelling of four-way coupling in particle-laden horizontal channel flow

Santiago Laín [1], Martin Sommerfeld *, Johannes Kussin

Institut für Verfahrenstechnik, Fachbereich Ingenieurwissenschaften, Martin-Luther-Universität Halle-Wittenberg, D-06099 Halle (Saale), Germany

Abstract

Detailed measurements in a horizontal channel flow laden with solid particles with different size and loading ratio were performed using phase-Doppler anemometry. The data were required for the validation of numerical calculations based on the Euler/Lagrange approach. In this approach the Reynolds-averaged continuity and Navier–Stokes equations in connection with a full Reynolds-stress model constitute the basis. The conservation equations include appropriate source terms resulting from the dispersed phase (i.e., two-way coupling). For modelling the particle phase in the Lagrangian frame all relevant effects are accounted for, such as, turbulent dispersion, transverse lift forces, wall collisions with roughness, and inter-particle collisions (i.e., often called four-way coupling). Comparison of measurement and numerical calculation is presented for different particle diameters and mass loading. The agreement was found to be reasonable good for both mean and fluctuating velocities.

1. Introduction

Confined gas–solid flows are frequently found in industrial and chemical process technology. As a result of the complex microphysical phenomena affecting the particle motion, such as turbulent dispersion, wall collisions, inter-particle collisions, and flow modulation by the particles, a reliable numerical prediction is rather sophisticated. An essential requirement are reliable experiments which may be used as a basis for model development and refinement and additionally for the validation of the numerical calculations. A number of experiments were performed in the past aiming at a detailed analysis of particulate flows in pipes and channels. A very detailed set of experiments was, for example, provided by Tsuji and Morikawa (1982, 1984) for a gas–solid flow in a horizontal and vertical pipe using different types of relatively large polystyrene spheres. Kulick et al. (1994) experimentally analysed a downward directed gas–solid flow in a channel of 40 mm height. The channel had a length of 5.2 m and a sophisticated feeding system was used in order to insure a homogeneous dispersion of the particles. The particles used in the experiment were Lycopodium, glass beads with different diameter, and copper beads. The main objective in this study was the analysis of turbulence modulation considering particle mass loadings up to about 0.5 (kg particles)/(kg air). Unfortunately, the experiments were not done carefully enough and it seems that a fully developed flow was not achieved, since particles were slower than the gas phase. This is caused by a change of wall material just above the measurement location and was demonstrated by a number of studies using LES (large eddy simulations, see for example Lei et al. (2001)) and DNS (direct numerical simulations). Detailed experiments in different elements of pipes with 80 and 150 mm diameter were performed using phase-Doppler anemometry (PDA) and a laser light sheet technique for particle concentration measurements by Huber and Sommerfeld (1998). The particles were again spherical glass beads with number mean diameters of 40 and 100 μm, respectively. A mass loading up to about 2 could be analysed in these studies. It was clearly demonstrated that wall roughness plays a significant role in the development of the particle concentration in different cross-sections of the pipe system.

* Corresponding author. Tel.: +49-3461-462-879; fax: +49-3461-462-878.

E-mail address: martin.sommerfeld@iw.uni-halle.de (M. Sommerfeld).

[1] Present address: Laboratory of Research in Combustion Technologies (LITEC), C/María de Luna 10, 50015 Zaragoza, Spain.

0142-727X/02/$ - see front matter
PII: S0142-727X(02)00160-1

Additionally, numerical calculations based on the Euler/Lagrange approach were performed. By accounting for wall roughness and inter-particle collisions good agreement with the measurements was achieved for the stainless steel and the glass pipe. Also the calculations by Lun and Liu (1997) and Lun (2000) were based on the Euler/Lagrange approach considering inter-particle collisions and wall collisions without roughness. Initially (Lun and Liu, 1997), a horizontal channel according to Tsuji et al. (1987) was considered. The results clearly revealed the importance of restitution ratio and friction coefficient in modelling inter-particle collisions. The second study (Lun, 2000) concentrated on modelling turbulence modulation for larger particles where wakes may result in a considerable enhancement of turbulence. On the basis of the experimental data of Wu and Faeth (1994), an empirical wake model was proposed. However, the agreement of the calculations for a vertical pipe (Tsuji and Morikawa, 1984) was found to be not very good.

One of the first studies where a full Reynolds-stress model with two-way coupling based on the standard terms was used for the prediction of gas-particle flows in a channel was introduced by Kohnen and Sommerfeld (1997). Additionally, a two-time-scale k–ε turbulence model was used and the predictions were compared with the data of Kulick et al. (1994). Recently, Berlemont and Achim (2001) analysed the effect of four-way coupling (i.e., inter-particle collisions) on the prediction of a vertical gas–solid flow (Tsuji and Morikawa, 1984) using the Euler/Lagrange approach with a Reynolds-stress turbulence model. It was demonstrated that the gas-phase fluctuating velocity components were considerably reduced due to the effect of inter-particle collisions.

In extension of the experimental studies previously performed in different pipes the present measurements are related to a detailed analysis of a gas–solid flow in a horizontal channel by considering also different degrees of wall roughness and varying the other parameters, such as, conveying velocity, particle mass loading, particle mean diameter, and size distribution (Kussin and Sommerfeld, 2001). These data are being used for the validation and improvement of the Euler/Lagrange approach using recently developed models on wall collisions (Sommerfeld and Huber, 1999) and inter-particle collisions (Sommerfeld, 2001).

2. Test facility

The entire test facility is shown in Fig. 1. The main component of the test facility is a horizontal channel of 6 m length which has a height of 35 and a width of 350 mm, so almost two-dimensional flow conditions can be established. The upper and lower channel walls were made of stainless steel plates which could be exchanged

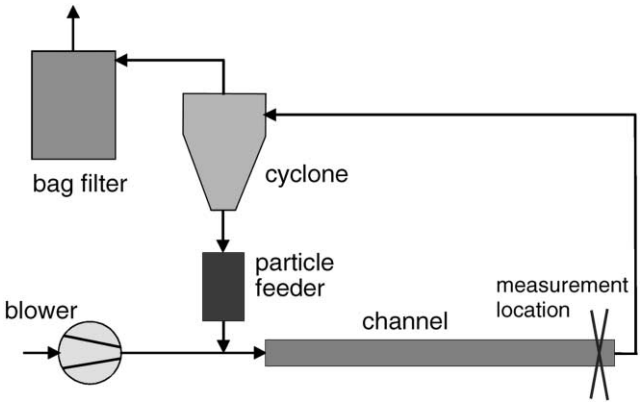

Fig. 1. Schematics of experimental facility.

in order to study the effect of wall material and wall roughness on the particle behaviour. The measurements were performed close to end of the channel at a distance of 5.8 m from the entrance. In order to allow optical access for the applied PDA, the side walls were made of glass plates and a glass window of 35 by 350 mm was inserted at the top wall. The required air flow rate was provide by two roots blowers mounted in parallel with nominal flow rates of 1002 and 507 m^3/h, respectively. The blowers are connected with the test section using a 130-mm pipe. Just prior to the channel a mixing chamber for injecting the particles and a flow conditioning section where the cross-section changes from circular to rectangular are mounted. Additionally, several sieves are inserted in this section in order to ensure rather homogeneous flow conditions at the entrance of the channel. In a straight section of 2 m before the mixing chamber a flow meter, and temperature, humidity, and pressure sensors are installed. For feeding the particle material into the mixing chamber a screw feeder is used, where the particle mass flow rate can be adjusted accordingly. In order to ensure a continuous particle feeding the air is injected into the mixing chamber through a converging nozzle, whereby a lower pressure is established. The resulting jet enters the exit pipe of the mixing chamber on the opposite side. At the end of the channel a 90°-bend is mounted which is connected to a flow passage where the cross-section changes from rectangular to circular. A flexible pipe is used for conveying the gas-particle mixture to a cyclone separator. The separated particles are re-injected into the reservoir of the particle feeder through a bucket wheel. Finally, the air from the cyclone passes through a bag-filter in order to remove also very fine particles (i.e. the tracer particles) and is released into the environment. The test facility described above allows for reach conveying velocities of up to 30 m/s and mass loadings up to 2 (kg dust)/(kg air) could be established.

The particles used in the experiment were spherical glass beads with different mean diameter $D_p = 60$, 100,

195, 625 and 1000 μm ($\rho_p = 2500$ kg/m^3). For allowing simultaneous measurements of the air and particle velocities, spherical tracer particles with a nominal size of 4 μm were added to the flow. This was done by mixing the tracers with the solid particles in the reservoire on the feeder. Hence, a discrimination between dispersed phase particles and tracer was possible using the method of Qiu et al. (1991) which is based on the signal phase discrimination. For the present experiments stainless steel walls with a mean roughness height of 4 and 7 μm were used respectively. Additional experimental results are presented by Kussin and Sommerfeld (2001).

3. Summary of numerical approach

The numerical calculations of the particle-laden gas flow in an horizontal channel have been performed using the Euler/Lagrange methodology. The fluid flow was calculated based on the Euler approach by solving the full Reynolds stress turbulence model equations extended in order to account for the effects of the dispersed phase (Kohnen and Sommerfeld, 1997).

The time-dependent conservation equations for the fluid may be written in the general form (in tensorial notation):

$$(\rho\phi)_{,t} + (\rho U_i\phi)_{,i} = (\Gamma_{ik}\phi_{,k})_{,i} + S_\phi + S_{\phi p} \tag{1}$$

where ρ is the gas density, U_i are the Reynolds-averaged velocity components, and Γ_{ik} is an effective transport tensor. The usual source terms within the continuous phase are summarised in S_ϕ, while $S_{\phi p}$ represents the additional source term due to phase interaction. Table 1 summarises the meaning of the quantities for the different variables ϕ, being P the mean pressure, μ the gas viscosity and $R_{jl} = \overline{u_j' u_l'}$ the components of the Reynolds stress tensor.

The calculation of the particle phase by the Lagrangian approach requires the solution of the equation of the motion for each computational particle. This equation includes the particle inertia, drag, gravity-buoyancy, slip-shear lift force and slip-rotational lift force. Other forces such as Basset history term, added mass and fluid inertia are negligible for high ratios of particle to gas densities. The change of the angular velocity along the particle trajectory results from the viscous interaction with the fluid (i.e., the torque $\vec{T}$). Hence, the equations of motion for the particles are given by

$$\frac{\mathrm{d}x_{p\,i}}{\mathrm{d}t} = u_{p\,i} \tag{2}$$

$$m_p \frac{\mathrm{d}u_{p\,i}}{\mathrm{d}t} = \frac{3}{4}\frac{\rho}{\rho_p D_p} m_p c_D (u_i - u_{p\,i})|\vec{u} - \vec{u}_B| + m_p g_i \left(1 - \frac{\rho}{\rho_p}\right) + F_{ls\,i} + F_{lr\,i} \tag{3}$$

$$I_p \frac{\mathrm{d}\omega_{p\,i}}{\mathrm{d}t} = T_i \tag{4}$$

Here, $x_{p\,i}$ are the coordinates of the particle position, $u_{p\,i}$ are its velocity components, $u_i = U_i + u_i'$ is the instantaneous velocity of the gas, D_p is the particle diameter and ρ_p is the density of the solids. The particle mass is given by $m_p = (\pi/6)\rho_p D_p^3$ and $I_p = 0.1 m_p D_p^2$ is the moment of inertia for a sphere. The drag coefficient is obtained using the standard correlation:

$$c_D = \begin{cases} 24 Re_p^{-1}(1 + 0.15 Re_p^{0.687}) & Re_p \leqslant 1000 \\ 0.44 & Re_p > 1000 \end{cases} \tag{5}$$

where $Re_p = \rho D_p |\vec{u} - \vec{u}_p|/\mu$ is the particle Reynolds number.

The slip-shear force is based on the analytical result of Saffman (1965) and extended for higher particle Reynolds numbers according to Mei (1992):

$$\vec{F}_{ls} = 1.615 D_p \mu Re_s^{1/2} c_{ls} \left[\left(\vec{u} - \vec{u}_p\right) \times \vec{\omega}\right] \tag{6}$$

where $\vec{\omega} = \nabla \times \vec{u}$ is the fluid rotation, $Re_s = \rho D_p^2 |\vec{\omega}|/\mu$ is the particle Reynolds number of the shear flow and $c_{ls} = F_{ls}/F_{ls,Saff}$ represents the ratio of the extended lift force to the Saffman force:

$$c_{ls} = \begin{cases} (1 - 0.3314\beta^{0.5})\mathrm{e}^{-Re_p/10} + 0.3314\beta^{0.5} & Re_p \leqslant 40 \\ 0.0524(\beta Re_p)^{0.5} & Re_p > 40 \end{cases} \tag{7}$$

and β is a parameter given by $\beta = 0.5 Re_s/Re_p$.

Table 1
Summary of terms in the general equation for the different variables that describe the gas phase

ϕ	Γ_{ik}	S_ϕ
1	0	0
U_j	$\mu\delta_{ik}$	$-P_{,j} + (\Gamma_{ik}U_{i,k})_{,i} - \rho R_{ij,i} + \rho g_j$
R_{jl}	$c_S \rho R_{ik} k/\varepsilon$	$\mathscr{P}_{jl} - \varepsilon_{jl} + \Pi_{jl}$
ε	$c_\varepsilon \rho R_{ik} k/\varepsilon$	$c_{\varepsilon 1}\mathscr{P}_{kk}\varepsilon/k - \rho c_{\varepsilon 2}\varepsilon^2/k$

$\mathscr{P}_{jl} = \rho(R_{jk}U_{l,k} + R_{lk}U_{j,k})$
$\varepsilon_{jl} = \frac{2}{3}\rho\delta_{jl}\varepsilon$
$\Pi_{jl} = -c_1\rho\frac{\varepsilon}{k}(R_{jl} - \frac{1}{3}\delta_{jl}R_{kk}) - c_2\rho(\mathscr{P}_{jl} - \frac{1}{3}\delta_{jl}\mathscr{P}_{kk})$
$c_S = 0.22;\ c_\varepsilon = 0.18;\ c_{\varepsilon 1} = 1.45$
$c_{\varepsilon 2} = 1.9;\ c_1 = 1.8;\ c_2 = 0.6$

The applied slip-rotational lift force is based on the relation given by Rubinow and Keller (1961), which was extended to account for the relative motion between particle and fluid. Moreover, recent measurements by Oesterlé and Bui Dinh (1998) allowed an extension of this lift force to higher particle Reynolds numbers. Hence, the following form of the slip-rotation lift force has been used

$$\vec{F}_{\mathrm{lr}} = \frac{\pi}{8} D_{\mathrm{p}}^3 \rho \frac{Re_{\mathrm{p}}}{Re_{\mathrm{r}}} c_{\mathrm{lr}} \left[\vec{\Omega} \times \left(\vec{u} - \vec{u}_{\mathrm{p}} \right) \right] \tag{8}$$

with $\vec{\Omega} = 0.5 \nabla \times \vec{u} - \vec{\omega}_{\mathrm{p}}$ and the Reynolds number of particle rotation is given by $Re_{\mathrm{r}} = \rho D_{\mathrm{p}}^2 |\vec{\Omega}| / \mu$. The lift coefficient according to Oesterlé and Bui Dinh (1998) is given for $Re_{\mathrm{p}} < 140$ by

$$c_{\mathrm{lr}} = 0.45 + \left(\frac{Re_{\mathrm{r}}}{Re_{\mathrm{p}}} - 0.45 \right) \mathrm{e}^{-0.05684 Re_{\mathrm{r}}^{0.4} Re_{\mathrm{p}}^{0.3}} \tag{9}$$

For the torque acting on a rotating particle the expression of Rubinow and Keller (1961) was extended to account for the relative motion between fluid and particle and higher Reynolds numbers

$$\vec{T} = \frac{\rho}{2} \left(\frac{D_{\mathrm{p}}}{2} \right)^5 c_{\mathrm{R}} |\vec{\Omega}| \vec{\Omega} \tag{10}$$

where the coefficient of rotation is obtained from Rubinow and Keller (1961) and direct numerical simulations of Dennis et al. (1980) in the following way:

$$c_{\mathrm{R}} = \begin{cases} \dfrac{64\pi}{Re_{\mathrm{r}}} & Re_{\mathrm{r}} \leqslant 32 \\ \dfrac{12.9}{Re_{\mathrm{r}}^{0.5}} + \dfrac{128.4}{Re_{\mathrm{r}}} & 32 < Re_{\mathrm{r}} < 1000 \end{cases} \tag{11}$$

Eqs. (2)–(4)). For sufficiently small time steps and assuming that the forces remain constant during this time step, the new particle location, the linear and angular velocities are calculated.

The instantaneous fluid velocity components at the particle location occurring in (3) are determined from the local mean fluid velocity interpolated from the neighbouring grid points and a fluctuating component generated by the Langevin model described by Sommerfeld et al. (1993). In this model the fluctuation velocity is composed of a correlated part from the previous time step and a random component sampled from a Gaussian distribution function. The correlated part is calculated using appropriate time and length scales of the turbulence form the Reynolds stress turbulence model.

When a particle collides with the wall, the wall collision model provides the new particle linear and angular velocities and the new location in the computational domain after rebound. The applied wall collision model, accounting for wall roughness, is described in Sommerfeld and Huber (1999). According to the presented experimental results the variation of the restitution (e_{w}, being defined as the absolute value of the ratio of the normal velocity components after collision to that before collision) and friction (μ_{w}) coefficients versus the impact angle α (expressed in degrees) for spherical particles is given by

$$e_{\mathrm{w}} = \max\{1 - 0.0136\alpha, 0.7\}$$

$$\mu_{\mathrm{w}} = \max\{1 - 0.0175\alpha, 0.15\}$$

The wall roughness seen by the particle is simulated assuming that the impact angle is composed of the particle trajectory angle plus a stochastic contribution due to wall roughness. The probability of this wall roughness angle can be approximated by a normal distribution function with standard deviation of $\Delta\gamma$. The value of $\Delta\gamma$ depends on the structure of the wall roughness and on the particle size. In the present calculations, the dependencies between $\Delta\gamma$ and D_{p} showed in Fig. 2 have been used, according to the experimental studies of Sommerfeld and Huber (1999).

Inter-particle collisions are modelled by the stochastic approach described in detail in Sommerfeld (2001). This model relies on the generation of a fictitious collision partner and accounts for a possible correlation of the velocities of colliding particles in turbulent flows. For the particle–particle collisions the restitution coefficient was taken as a constant equal to 0.9 and the static and dynamic friction coefficients were made equal to 0.4.

Since inter-particle collisions will modify the particle phase properties and eventually the gas phase, the consideration of this combined effect is often referred to as four-way coupling.

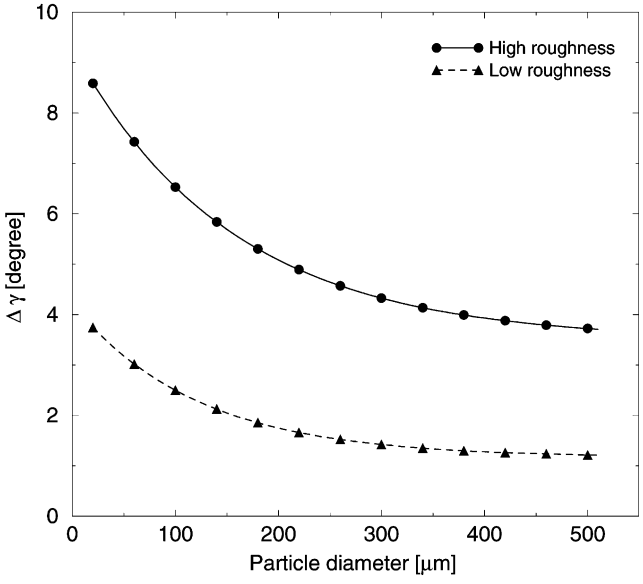

Fig. 2. Values of $\Delta\gamma$ versus particle diameter D_{p} for the two roughness cases considered.

4. Effect of particles on gas flow

The standard expression for the momentum equation source term due to the particles has been used. It is obtained by time and ensemble averaging for each control volume in the following form:

$$\overline{S_{U_i\mathrm{p}}} = -\frac{1}{V_{\mathrm{cv}}}\sum_k m_k N_k \times \sum_n \left\{ \left(\left[u_{\mathrm{p}\,i}\right]_k^{n+1} - \left[u_{\mathrm{p}\,i}\right]_k^{n} \right) - g_i \left(1 - \frac{\rho}{\rho_{\mathrm{p}}}\right) \Delta t_{\mathrm{L}} \right\} \tag{12}$$

where the sum over n indicates averaging along the particle trajectory (time averaging) and the sum over k is related to the number of computational particles passing the considered control volume with the volume V_{cv}. The mass of an individual particle is m_k and N_k is the number of real particles in one computational particle. Δt_{L} is the Lagrangian time step which is used in the solution of (3).

The source terms in the conservation equations of the Reynolds stress components, R_{jl}, are expressed in the Reynolds average procedure as:

$$S_{R_{jl}\mathrm{p}} = \overline{u_j S_{U_l\mathrm{p}}} + \overline{u_l S_{U_j\mathrm{p}}} - \left(U_j \overline{S_{U_l\mathrm{p}}} + U_l \overline{S_{U_j\mathrm{p}}}\right) \tag{13}$$

while the source term in the ε-equation is modelled in the standard way

$$S_{\varepsilon\mathrm{p}} = C_{\varepsilon 3}\frac{1}{2}\frac{\varepsilon}{k} S_{R_{jj}\mathrm{p}} \tag{14}$$

with $C_{\varepsilon 3} = 1.0$ and the sum is implicit in the repeated subindex j.

All the calculations have been performed with a mesh of 800×40 control volumes in the horizontal and vertical direction, respectively. Such a resolution was found to be sufficient for producing grid-independent results. A converged solution of the coupled two-phase flow system is obtained by successive solution of the Eulerian and Lagrangian part, respectively. Initially, the flow field is calculated without particle phase source terms until a converged solution is achieved. Thereafter, a large number of parcels are tracked through the flow field (typically 20000) and the source terms are sampled. In this first Lagrangian calculation inter-particle collisions are not calculated, since the required particle phase properties are not yet available. Hence, for each control volume the particle concentration, the local particle size distribution and the size-velocity correlations for the mean velocities and the rms-values are sampled. The particle phase properties are sampled in the standard way for each transverse cell when the computational particle crosses this location. These properties are updated each Lagrangian iteration in order to allow correct calculation of inter-particle collisions. From the second Eulerian calculation, the source terms of the dispersed phase are introduced using an under-relaxation procedure (Kohnen et al., 1994). For the present calculations typically about 30 coupling iterations have been performed with an under-relaxation factor of 0.25.

5. Results

The numerical calculations have been compared with experimental data obtained in the horizontal channel facility described in the first section. Three particle diameters have been considered, i.e. $D_{\mathrm{p}} = 60$, 100, 195 μm. The particle material density was $\rho_{\mathrm{p}} = 2500\ \mathrm{kg\,m^{-3}}$ (i.e., spherical glass beads). For the 60 μm particles the size distribution was accounted for according to the measurements. The size distribution was resolved by six equidistant classes between 33 and 83 μm. The larger particles could be considered to be mono-disperse due to the narrow size distribution and the resulting small value of the standard deviation normalised by the mean particle diameter, implying that the particle response characteristics are quite similar for the largest and smallest particles in the distribution. The simulations have been performed using the full Reynolds stress turbulence model described in the previous section accounting for particle-wall and inter-particle collisions, i.e. considering the so-called four-way coupling. Two configurations have been selected:

1. *Case 1:* High roughness, corresponding to the upper curve $\Delta\gamma(D_{\mathrm{p}})$ in Fig. 2, and high gas mean velocity, $U_0 = 19.5\ \mathrm{m\,s^{-1}}$.
2. *Case 2:* Low roughness, corresponding to the lower curve $\Delta\gamma(D_{\mathrm{p}})$ in Fig. 2, and lower gas mean velocity, $U_0 = 14.25\ \mathrm{m\,s^{-1}}$.

The gas density and the dynamic viscosity were $\rho = 1.16\ \mathrm{kg\,m^{-3}}$ and $\mu = 1.8 \times 10^{-5}\ \mathrm{kg\,m^{-1}\,s^{-1}}$, respectively. In the following, all the comparisons between experimental data and calculations are showed in the measuring location $x = 5.8$ m downstream the inlet.

Fig. 3 shows the effect of particle mass loading (LR = 0.2, 0.5, 0.7) on the gas-phase velocities in the case of 100 μm particles and high roughness (Case 1) in comparison to the measurements. The profiles of the calculated mean gas velocity in the horizontal direction reveal that with increasing loading and inter-particle collision frequency a reduction of the gas velocity outside the core of the channel occurs. Hence, the profiles become slightly more spiky. Moreover, both components of the mean fluctuating velocity, horizontal u' and vertical v', are reduced regarding the single-phase flow, which is consistent with the observation that small particles tend to suppress turbulence. For the vertical component this decay is more pronounced and rather symmetric. In the experiments, however, the vertical velocity fluctuation of the gas is more or less constant

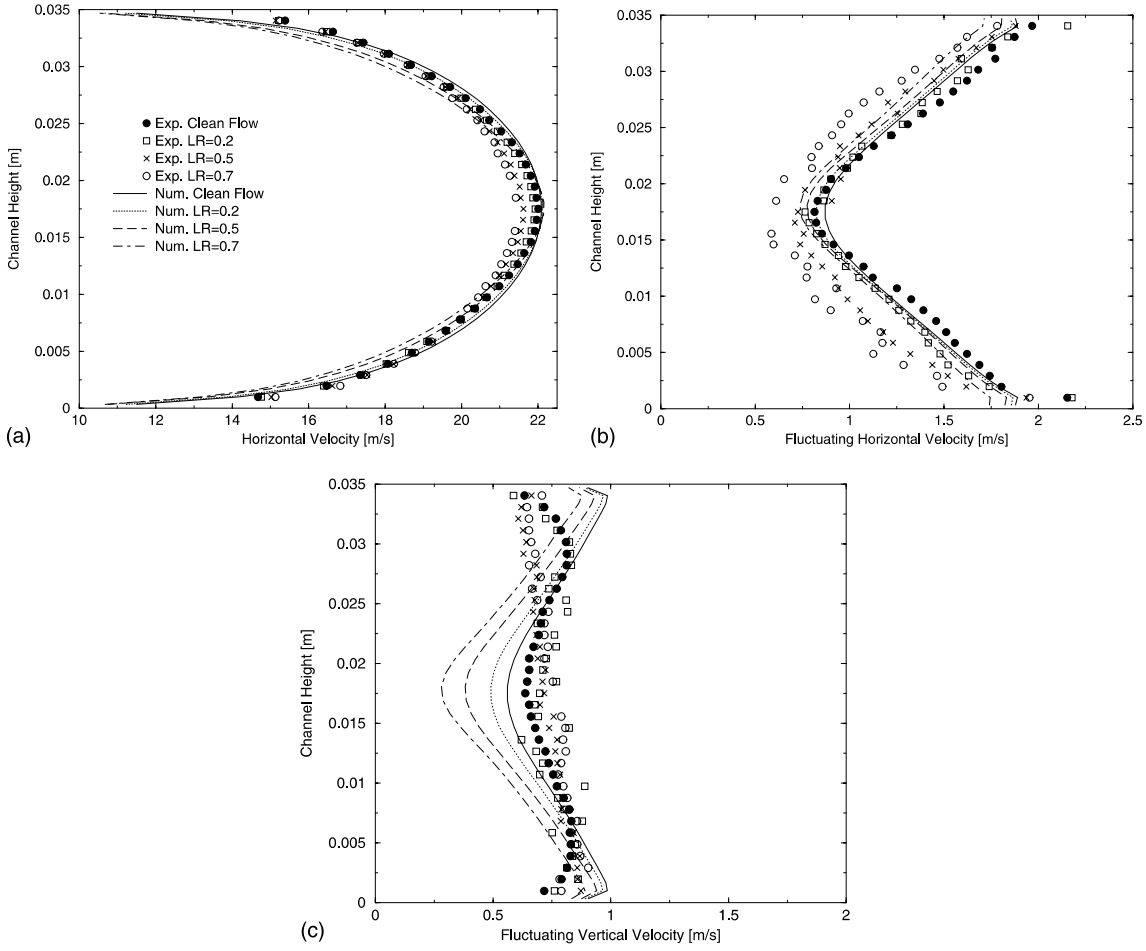

Fig. 3. Effect of the particle mass loading on the gas velocity profiles for a particle diameter of 100 μm, calculations with inter-particle collisions (i.e., four-way coupling) and for high roughness (Case 1). Horizontal mean velocity (top left), rms horizontal velocity (top right) and rms vertical velocity (bottom).

and no pronounced damping with increasing loading is observed.

The calculated horizontal component of the gas phase fluctuations shows a lower decay compared to the vertical one. Since the collision frequency is higher in the lower part of the channel due to the influence of gravitational settling, also the horizontal gas-phase fluctuation velocity is not so strongly reduced than in the upper half when particle loading is increased (Fig. 3). The experiments show a somewhat stronger decay of the horizontal velocity fluctuation with increasing particle loading, but the shape of the profiles is very similar to the calculations. As shown in Fig. 4 the turbulent kinetic energy is reduced with increasing loading when accounting for two-way coupling only. The consideration of inter-particle collisions causes again a slight enhancement of turbulence, which is consistent with the profiles of the gas phase horizontal fluctuation. Due to the different modulation of the gas phase fluctuating components, the turbulence structure becomes more anisotropic with increasing particle mass loading (Fig. 4).

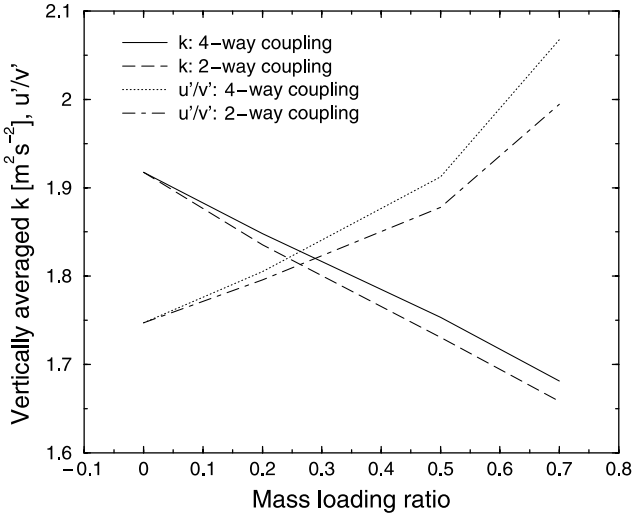

Fig. 4. Variation of the vertically averaged (i.e., across the channel) gas phase turbulent energy and ratio of the fluctuating components with increasing particle mass loading (100 μm diameter particles, high roughness and high conveying velocity, Case 1).

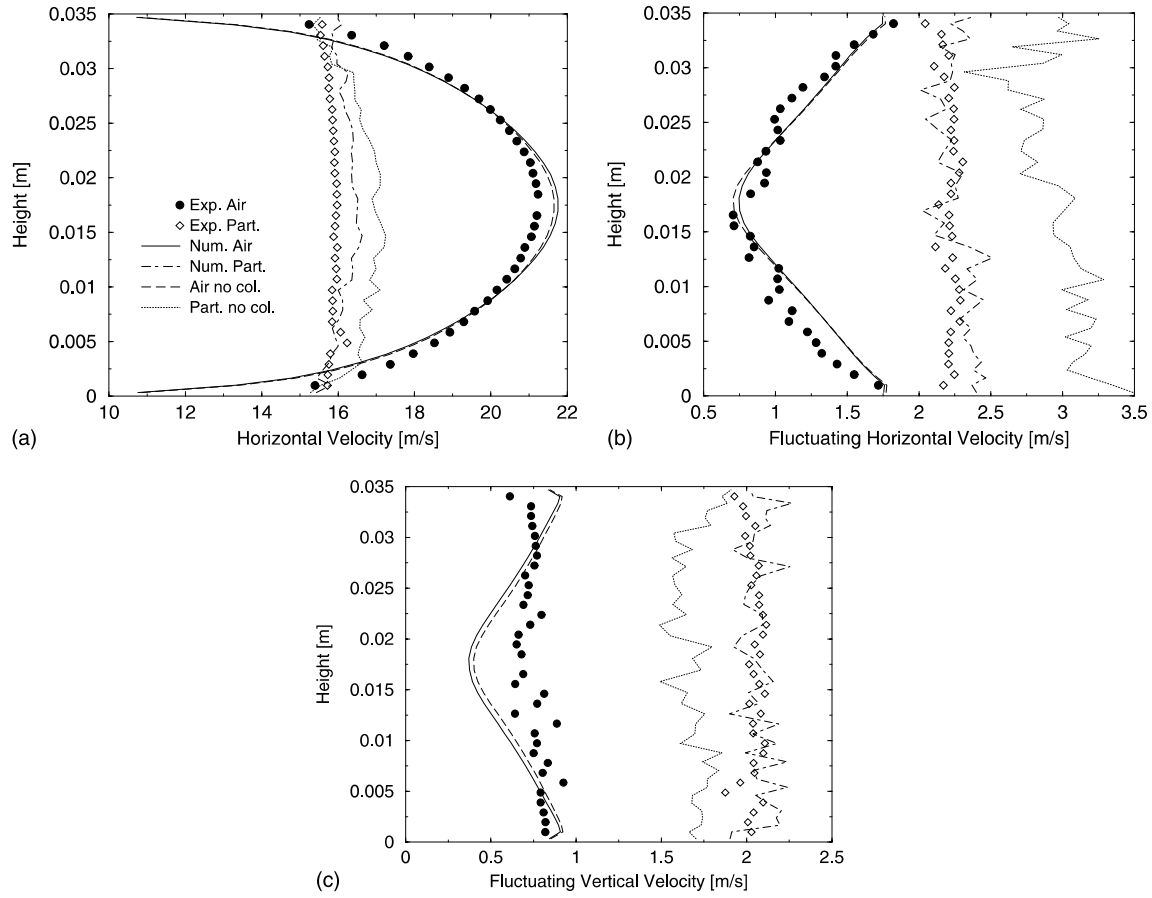

Fig. 5. Comparison of measurements and calculation for the $D_p = 195$ μm particles with LR = 1.0 and high roughness (Case 1). Horizontal mean velocity (top left), rms horizontal velocity (top right) and rms vertical velocity (bottom). Also the simulations without considering inter-particle collisions (i.e., with two-way coupling) are included.

With inter-particle collisions, this effect becomes even slightly stronger.

In Fig. 5 the results for 195 μm particles and high roughness (Case 1) are presented with loading ratio LR = 1.0. Two-way and four-way coupling calculations are shown versus the experimental data for the mean horizontal and both rms velocity components. The gas-phase predictions are in reasonable agreement with the measurements. For the vertical fluctuation some difference in the shape of the profile is observed similar to the result presented in Fig. 3. The calculated profile shows a distribution similar to that known for a single phase channel flow. However, the measurements provide almost constant values across the channel. This difference is attributed to problems in accurately measuring the transverse component of the gas phase. The particles properties show quite good agreement with the experimental data, even with the vertical rms velocity component, when the four-way coupling is considered. If only the two-way coupling is taken into account, i.e. neglecting inter-particle collisions, an over-prediction of the particles horizontal fluctuating and mean velocities is observed as well as an underestimation of the vertical rms velocity values. These findings are associated with the following effects:

- Inter-particle collisions increase the wall collision frequency for larger particles resulting in a higher momentum loss due to wall collisions and hence a reduction of the mean particle velocity.
- As a consequence of inter-particle collisions a redistribution of the fluctuating components occurs, namely the streamwise component is reduced while the normal component is enhanced. This implies an isotropisation of the particle phase fluctuating motion.

Both effects are very well captured by the calculations and agree with previous observations (Sommerfeld, 1998; Sommerfeld et al., 2001).

Fig. 6 shows the comparison for the smaller particles with loading ratio of 0.2, also for high roughness and high conveying velocity (Case 1). In this case the particle size distribution is very important and was considered in the calculations in accordance with the experiments. For the gas phase the agreement between measurement and

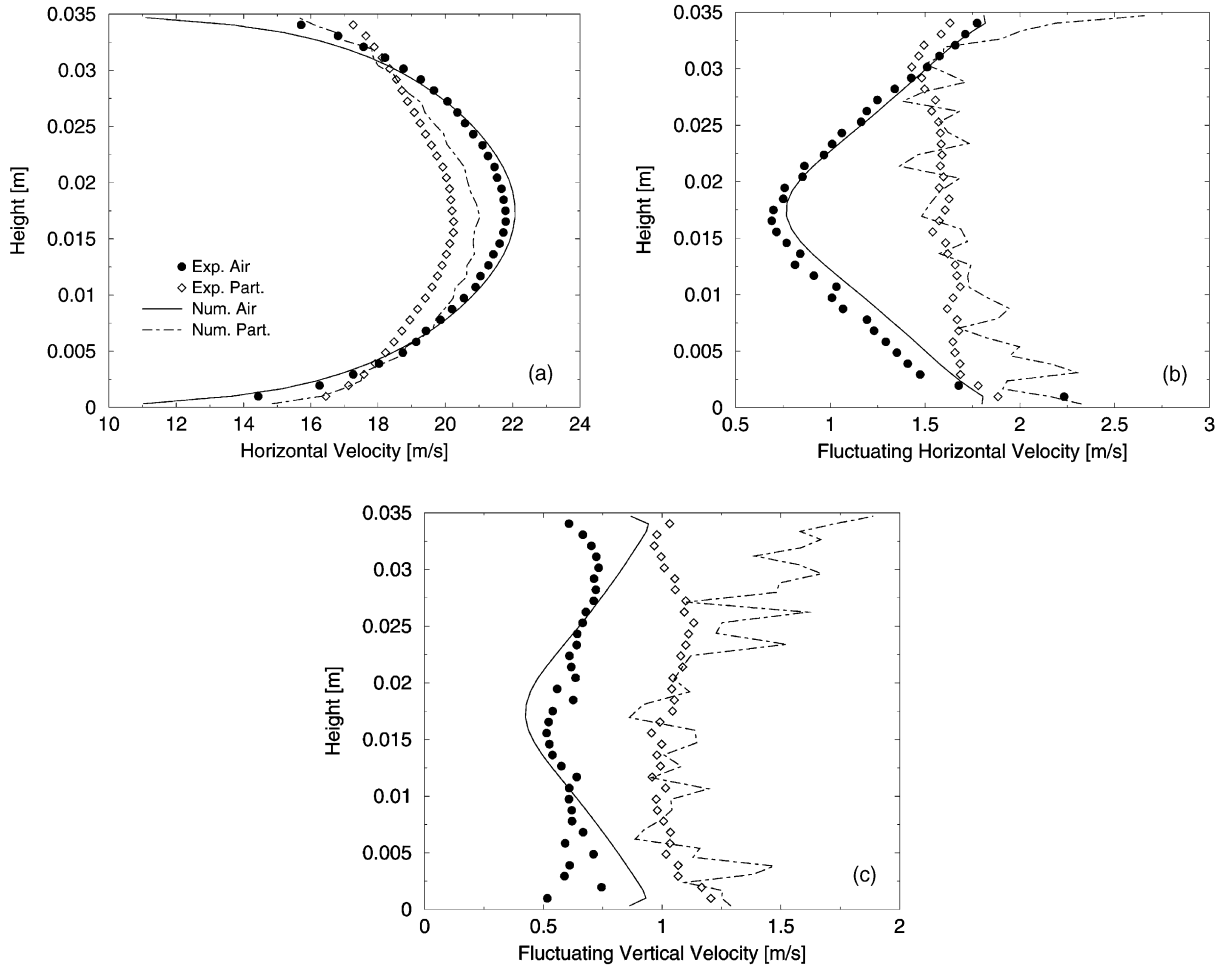

Fig. 6. Comparison of measurement and calculation for particles with $D_p = 60$ μm (with particle size distribution and four-way coupling), LR = 0.2 and high roughness (Case 1). Horizontal mean velocity (top left), rms horizontal velocity (top right) and rms vertical velocity (bottom).

calculation is again reasonably good. For this case the particle mean horizontal velocity (top left) is slightly overestimated compared to the measurements, while the corresponding rms values (top right) are reasonably well captured. The bottom graphic in Fig. 6 shows the comparison for the vertical velocity rms values, where the simulations provide similar results to the experiments for the particles in the lower two thirds of the channel, while there is an over-prediction in the upper third. This effect can be explained because in the upper regions of the channel the number density of particles is smaller than in the lower parts leading to a larger values of the rms components of the velocity.

Fig. 7 presents results for the low roughness and low conveying velocity (Case 2), where the diameter of the particles was 100 μm and the loading ratio 0.9. As a result of the lower conveying velocity, gravitational settling is more pronounced, which is revealed by the profiles of the normalised particle mass flux. This also causes a stronger asymmetry in the four-way coupling effects for the gas phase fluctuations. It is obvious that inter-particle collisions tend to enhance the gas phase fluctuation in the lower half of the channel, while a decay is observed in the upper half. The horizontal component of the gas phase mean velocity is only slightly influenced due to four-way coupling. The effects of inter-particle collisions on the particle-phase velocities are similar to the high velocity case (Fig. 5). Especially, for the horizontal component of the particle fluctuating velocity a high degree of asymmetry in the profiles is found. This is similar to the experimental observation and is a result of the considerable higher inter-particle collision frequencies in the lower half of the channel. Hence, also the velocity profiles for the particle phase mean and fluctuating velocities are stronger influenced in the lower half of the channel when accounting for inter-particle collisions. The horizontal particle phase fluctuation is remarkably reduced in the lower half of the channel and slightly enhanced in the upper half. The difference from the measured fluctuation may be attributed to some small changes in the wall roughness structure during the experiments. On the other

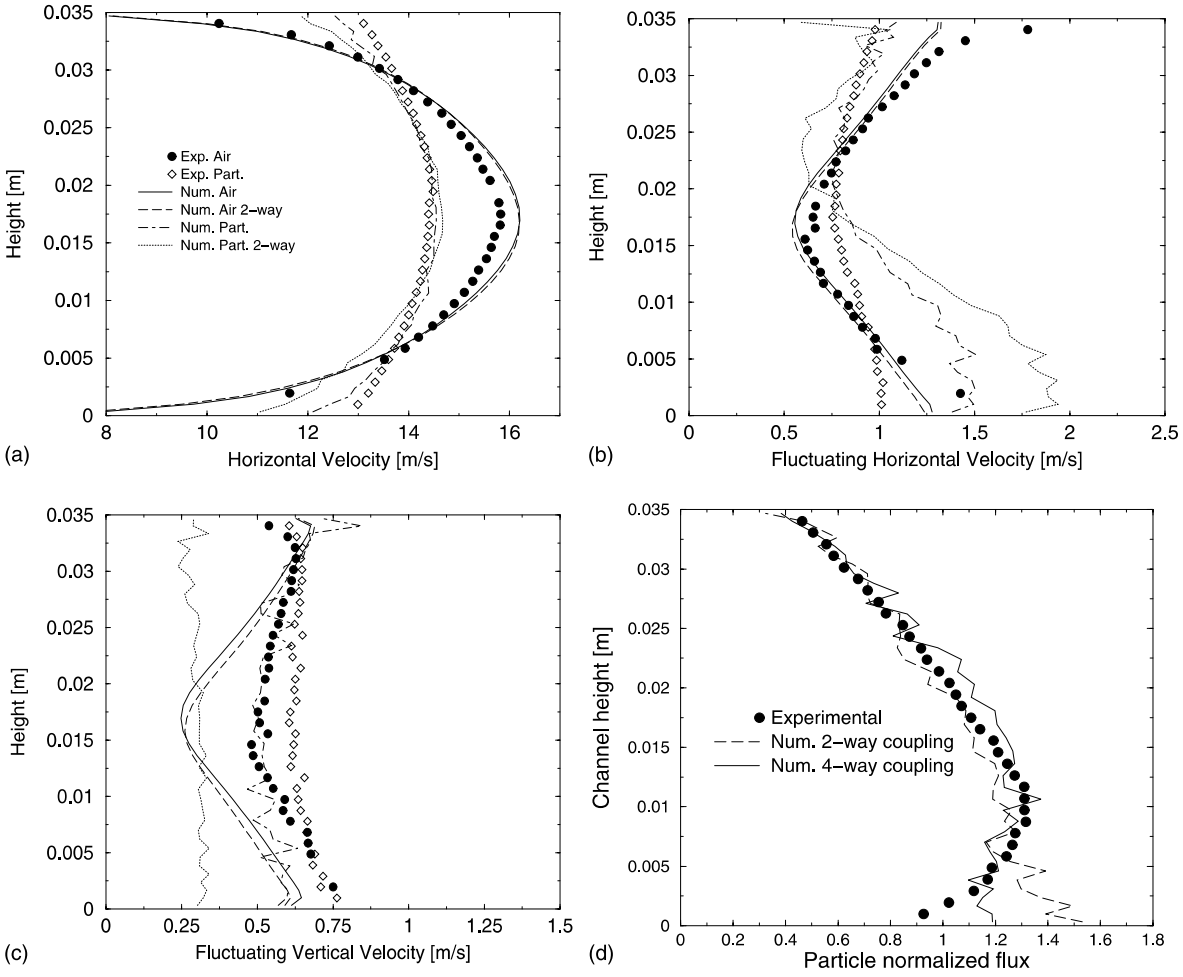

Fig. 7. Radial profiles for the different variables at $x = 5.8$ m in the channel flow. $D_p = 100$ μm, LR = 0.9 and low roughness with low velocity. Horizontal mean velocity (top left), horizontal rms velocity (top right), vertical rms velocity (bottom left) and normalized particle flux (bottom right).

hand, the vertical component is enhanced over the entire channel due to inter-particle collisions.

Finally, the vertical profiles of the normalised profiles of the particle mass flux reveal the redispersion effect due to particle collisions which is coupled with an enhancement of the vertical fluctuating component. The agreement with the measurements for the flux is satisfactory. This result again reveals the importance of inter-particle collisions on the particle phase properties even for moderate loading, especially when wall roughness effects are less pronounced.

6. Conclusion

This paper shows that the use of the Reynolds stress turbulence model in conjunction with a wall roughness model and a stochastic inter-particle model is appropriate enough to predict the behaviour of particle-laden turbulent gas flow in channels. Not only the mean but also rms particle velocities have been taken into account showing reasonably good agreement with detailed experimental measurements carried out using PDA.

Both, inter-particle collisions and wall roughness have a very strong effect on the development of the particle phase properties. The redistribution of the particle mean fluctuating components due to particle collisions and the resulting isotropisation of the fluctuating motion have been demonstrated. Additionally, the effect of inter-particle collisions on the gas-phase properties, i.e., the so-called four-way coupling has been analysed. A slight enhancement of the turbulent kinetic energy was caused by particle collisions.

The future work will be devoted to deal with larger particles as well as the evaluation of pressure drop in the channel.

Acknowledgements

The research project is financially supported by the Deutsche Forschungsgemeinschaft under contract

number So 204/12–1 and 2, which is gratefully acknowledged. Also, we gratefully acknowledge Dr. G. Kohnen for his useful comments and suggestions.

References

Berlemont, A., Achim, P., 2001. Influence of the isotropization of particle motion due to collisions on the fluid turbulence anisotropy in a turbulent pipe flow. 4th International Conference on Multiphase Flow, ICMF 2001, New Orleans, USA, Paper No. 354.

Dennis, S.C.R., Singh, S.N., Ingham, D.B., 1980. The steady flow due to a rotating sphere at low and moderate Reynolds numbers. J. Fluid Mech. 101, 257–279.

Huber, N., Sommerfed, M., 1998. Modelling and numerical calculation of dilute-phase pneumatic conveying in pipe systems. Powder Technol. 99, 90–101.

Kohnen, G., Rüger, M., Sommerfeld, M., 1994. Convergence behaviour for numerical calculations by the Euler/Lagrange method for strongly coupled phases. In: Crowe et al. (Ed.), Num. Meth. for Multiphase Flows, FED vol. 185, pp. 191–202.

Kohnen, G., Sommerfeld, M., 1997. In: The effect of turbulence modelling on turbulence modification in two-phase flows using the Euler-Lagrange approach. Proceedings of the 11th Symposium on Turbulent Shear Flows, vol. 2, P3. Grenoble, France, pp. 23–28.

Kulick, J.D., Fessler, J.R., Eaton, J.K., 1994. Particle response and turbulence modifikation in fully developed channel flow. J. Fluid Mech. 277, 109–134.

Kussin, J., Sommerfeld, M., 2001. Investigation of particle behaviour and turbulence modification in particle-laden channel flow. International Congress for Particle Technology, PARTEC 2001, Paper No. 046.

Lei, K., Taniguchi, N., Kobayashi, T., 2001. Full way coupling of large eddy simulation for particle-laden turbulent flows using new dynamic SGS models. Proceedings Turbulence and Shear Flow Phenomena, 2nd International Symposium, Stockholm, Sweden.

Lun, C.K.K., Liu, H.S., 1997. Numerical simulation of dilute turbulent gas–solid flows in horizontal channels. Int. J. Multiphase Flow 23, 575–605.

Lun, C.K.K., 2000. Numerical simulation of dilute turbulent gas–solid flows. Int. J. Multiphase Flow 26, 1707–1736.

Mei, R., 1992. An approximate expression for the shear lift force on a spherical particle at finite Reynolds number. Int. J. Multiphase Flow 18, 145–147.

Oesterlé, B., Bui Dinh, T., 1998. Experiments on the lift of a spinning sphere in a range of intermediate Reynolds numbers. Exp. Fluids 25, 16–22.

Qiu, H.H., Sommerfeld, M., Durst, F., 1991. High-resolution data processing for phase-Doppler measurements in a complex two-phase flow. Measurement Sci. Technol. 2, 455–463.

Rubinow, S.I., Keller, J.B., 1961. The transverse force on a spinning sphere moving in a viscous liquid. J. Fluid Mech. 11, 447–459.

Saffman, P.G., 1965. The lift on a small sphere in a shear flow. J. Fluid Mech. 22, 385–400.

Sommerfeld, M., Kohnen, G., Rüger, M., 1993. Some open questions and inconsistencies of Lagrangian particle dispersion models. Proceedings, 9th Symposium on Turbulent Shear Flows, Kyoto, Japan, Paper 15–1.

Sommerfeld, M., Huber, N., 1999. Experimental analysis and modelling of particle-wall collisions. Int. J. Multiphase Flow 25, 1457–1489.

Sommerfeld, M., 1998. Modelling and numerical calculation of turbulent gas–solid flows with the Euler/Lagrange approach. KONA (Powder and Particle), Number 16, pp. 194–206.

Sommerfeld, M., 2001. Analysis of inter-particle collisions in homogeneous isotropic turbulence using a stochastic Lagrangian modelling approach. Int. J. Multiphase Flow 27, 1829–1858.

Sommerfeld, M., Laín, S., Kussin, J., 2001. Analysis of transport effects of turbulent gas-particle flow in a horizontal channel. Proceedings of the 4th International Conference on Multiphase Flow, ICMF 2001, New Orleans, USA, Paper No. 520.

Tsuji, Y., Morikawa, Y., 1982. LDV measurements of an air-solid two-phase flow in a horizontal pipe. J. Fluid Mech. 120, 385–409.

Tsuji, Y., Morikawa, Y., 1984. LDV measurements of an air–solid two-phase flow in a vertical pipe. J. Fluid Mech. 139, 417–434.

Tsuji, Y., Morikawa, Y., Tanaka, T., Nakatsukasa, N., Nakatani, M., 1987. Numerical simulation of gas–solid two-phase flow in a two-dimensional horizontal channel. Int. J. Multiphase Flow 13, 671–684.

Wu, J.S., Faeth, G.M., 1994. Sphere wakes at moderate Reynolds numbers in a turbulent environment. AAIA J. 32, 535–541.